INTERNATIONAL JOURNAL OF CLIMATOLOGY
Int. J. Climatol. (2010)
Published online in Wiley Online Library
(wileyonlinelibrary.com) DOI: 10.1002/joc.2257

RMetS
Royal Meteorological Society

Exceedance of heat index thresholds for 15 regions under a warming climate using the wet-bulb globe temperature†

Katharine M. Willett[a,c]* and Steven Sherwood[b,c]
[a] *Met Office Hadley Centre, FitzRoy Road, Exeter, EX1 3PB, UK*
[b] *University of New South Wales, Sydney, Australia*
[c] *Department of Geology and Geophysics, Yale University, New Haven, CT 06511, USA*

ABSTRACT: Thermal comfort is quantified in 15 regions using the wet-bulb globe temperature (WBGT), examining past and future rates of thresholds exceedance corresponding to moderate, high, and extreme heat (28, 32, and 35 °C, respectively). As recent changes to thermal comfort appear to be dominated by temperature and humidity, a WBGT approximation based only on these is used. A new homogenised dataset from 1973 to 2003 is developed which provides WBGT daily means, daily maximums averaged over 5-day periods, and the highest extreme for each 5-day period; recent trends are positive for all regions except northeast USA and northeast Australia. A simple model for predicting summertime threshold exceedance rates, with a fixed distribution of anomalies about the seasonal mean, is found to adequately predict changes for the above quantities given seasonal mean values. This model is used to predict the impact of regional 1–5 °C temperature increases on WBGT exceedance rates with no change in relative humidity. Results show that heat events may worsen as much, or more, in humid tropical and mid-latitude regions even if they warm less than the global average, due to greater absolute humidity increases. A further 2 °C warming from the present is sufficient to push peak WBGT above 35 °C, an extreme heat event, in all regions except the UK.

An ensemble of HadCM3 climate model simulations is used to investigate likely regional changes in mean summertime temperature, relative humidity and WBGT under an A1B scenario for the 2020s and 2050s. Unsurprisingly, simulated regional changes often depart significantly from the global average, and the impact of regional changes in relative humidity is not always negligible. Increases in WBGT are nonetheless expected in all regions, and are more predictable than increases in temperature at least in mid-latitude regions owing to the compensating effects of humidity. © Royal Meteorological Society and Crown Copyright 2010.

KEY WORDS heat stress; humidity; climate change; wet-bulb globe temperature

Received 9 December 2009; Revised 15 October 2010; Accepted 15 October 2010

1. Introduction

There has been an overall moistening of the globe in recent decades, both near the ground (Dai, 2006; Willett *et al*., 2008 – henceforth W08) and aloft (Trenberth *et al*., 2005; Wentz *et al*., 2007). This is linked to increasing temperatures and is attributable, at least in part, to human causes (Willett *et al*., 2007; Santer *et al*., 2007). Rising absolute humidity in the lower troposphere has substantial implications for human thermal comfort and heat-related mortality and morbidity (Yaglou & Minard, 1957; Davis *et al*., 2003; Sparks *et al*., 2002; Kjellstrom *et al*., 2008; Margolis *et al*., 2006).

Many national weather centres (i.e. US, Australia, New Zealand, Canada, Germany) now regularly show a combined temperature and humidity index of some form, and substantial research efforts are being made to this effect in many countries (Air mass index, USA - Knight *et al*., 2008; Shanghai/China MHEWS – http://www.wmo.ch/pages/prog/drr/transfer/NWS/; COST 730 Universal Thermal Climate Index, Europe – www.utci.org). However, to date, there has been very little work, if any, focusing on combined temperature and humidity heat extremes, and climate change within the now well established 'extremes' community (Alexander *et al*., 2006; Gleason *et al*., 2008; Kenyon and Hegerl, 2008; O'neill and Ebi, 2009). There have been interdisciplinary efforts within the epidemiological community to investigate relationships between temperature, humidity, and Health Service mortality, as well as hospital admissions data (Hajat *et al*., 2006; Kovats *et al*., 2007; Kovats & Hajat, 2008; Barnett *et al*., 2010). Conclusions from these are mixed: humidity appears to be of importance in some cities/demographic groups but not others. The majority of such studies consider the relative humidity and composite indices where humidity contributes only a small proportion (0.3–0.7% in the various Apparent Temperature equations – Steadman, 1984). The use of absolute measures of humidity, or different indices, could

* Correspondence to: Katharine M. Willett, Met Office Hadley Centre, FitzRoy Road, Exeter EX1 3PB, UK.
E-mail: kate.willett@metoffice.gov.uk
† The contribution of K. M. Willett was written in the course of her employment at the Met Office, UK and is published with the permission of the Controller of HMSO and the Queen's Printer for Scotland.

prove useful. Indeed, thinking from the thermobiological community suggests that use of sophisticated indices incorporating humidity and including physiological models may reveal stronger links (G. Havenith *pers. comm.*).

Heat-related mortality is already thought to be the leading cause of death among meteorological phenomena in the US (Davis *et al*., 2003; Borden and Cutter, 2008). This includes classical heat stress in addition to heat-induced episodes of pre-existing illnesses (i.e. respiratory, cardio-vascular, nervous system disorders, etc. (Mastrangelo *et al*., 2006; Ishigami *et al*., 2008; O'neill and Ebi, 2009)) typically in the very old, very young, and those with a history of ill health (Falk, 1998; Davis *et al*., 2003; Donaldson *et al*., 2003). The very old and very young cannot thermo-regulate their bodies in extremes of heat very well and may be dependent on others to provide food, water, and cool surroundings. Extended periods (a few days) of high heat causes stress on the body to accumulate. This is exacerbated by sleep deprivation during warm nights. Urban environments can exacerbate this, especially at night when the urban heat island is most prevalent (Grimmond, 2007). With a growing global population, an increasing proportion of urban dwellers (now 50% (UNFPA, 2007)) and climate change, the heat-stress burden on society is set to increase considerably.

For obvious reasons, human tests can only be done on fit healthy adults, and so our understanding of how the humidity component of heat affects the very old, very young, and those with ill health is limited. For these people a more sedentary and indoor lifestyle is likely, so humidity may be of less importance. Thermobiological research on the physiological effects of heat on fit and healthy people does include humidity almost without exception, and in many cases, radiation and windspeed (Yaglou and Minard, 1957; Wallace *et al*., 2006; Katavoutas *et al*., 2009). Radiation, both long-wave and short-wave, directly applies heat to the body (Hoppe, 1999; Taylor, 2006). Windspeed is complex; it has a cooling effect for the most part but has been found to exacerbate heat stress at high temperatures due to dehydration. High absolute humidity conditions lead to higher relative humidity very close to the skin, therefore reducing the efficiency with which the body can evaporate sweat to maintain a safe core temperature.

The concept of thresholds to quantify sensible physical work loads is commonplace within military and athletics communities (see examples below). If heat extremes increase in either severity or frequency this will have a considerable knock-on effect on the productivity and safety of manual labour (Taylor, 2006; Kjellstrom *et al*., 2008), military operations, and sporting events. The Australian Open Tennis event in January 2009 was an interesting recent example where excessive heat caused heat-related injuries and withdrawals from the tournament by some of the contestants, before triggering action by local authorities.

Global temperatures are very likely to continue rising into the foreseeable future (IPCC, 2007). Following the Clausius-Clapeyron theory and recent trends (W08) it is reasonable to assume that absolute humidity will continue to increase over large portions of the globe. Given that recent and future increases (in frequency, severity, and longevity) in high-temperature extremes are documented (Gleason *et al*., 2008; Meehl and Tebaldi, 2004; IPCC, 2007) it is essential to quantify if and how heat extremes incorporating a humidity component are changing, and what future expectations might be. Henceforth, the term 'heat' refers to a combined temperature and humidity measure.

It is necessary to increase our understanding of the frequency and severity of both *extreme single event* and *extended period* heat to address exertional and occupational heat stress, classical heat stress and heat-related mortality. This will enable improved preparation for detrimental health and economic impacts from high heat extremes and give some idea of the challenges to be faced in the future, both for the vulnerable (very old, very young, and of ill-health), and the active population.

To address the above issues, summertime exceedances of heat thresholds in the contiguous US, Australia, Europe, the Caribbean, India, and Eastern China are investigated. First, the most common heat indices are described in Section 2 and the wet-bulb globe temperature WBGT validated as suitable for purpose. The data source and data formatting procedure is also discussed here. In Section 3, current WBGT climatology and recent threshold exceedance is quantified. Section 4 describes the creation of a simple model derived from past exceedance which is used to project future heat exceedances given various levels of background climate warming. Section 5 presents an analysis of the modelled exceedances for the 15 regions. This provides implications for future expectations of climate change impacts from heat stress. Section 6 discusses the broader issues and draws conclusions.

2. Methodology

2.1. Choosing a thermal comfort index

Relating atmospheric state to physiological comfort is no simple matter. Thermal comfort depends on age, health (including general healthiness, weight, and fitness), gender, level of activity, amount of clothing, acclimatisation, and also individual tolerance (Falk, 1998; SMA). Furthermore, there is no universally used method of quantifying thermal comfort. There are numerous heat indices both historical and in current use, varying widely in their level of complexity, input parameters, parameter weightings, humidity reference state (dry, moderate, or very humid), physiological assumptions (i.e. a person of average height, weight, health, and in moderate clothing), and intended end-user. All use temperature and humidity, but some include wind and radiation effects. An assorted list of indices is given in Table I.

An approximation to the WBGT is chosen for this study. The WBGT is the ISO standard for quantifying thermal comfort (ISO, 1989) and is currently in use by a number of bodies including the US and UK

Table I. Variables used to infer a thermal comfort quantity. T = air temperature (usually °C), (°C), T_{nwb} = natural wet-bulb temperature (°C), T_g = black globe temperature (°C), e = vapour pressure (hPa), q = specific humidity (g kg^{-1}), RH = relative humidity (%), SR = solar radiation (W m^{-2}), u = windspeed (m s^{-1}).

Variable	Input variables	Formula	Source
Apparent temperature for shaded conditions (T_a) (Equations exist for exposed, shaded and indoor conditions)	T, e, u	$T_a = T + 0.33e - 0.70u - 4.00$	Steadman, 1994 (in his eqn (1)
Heat index (HI)	T in Fahrenheit, RH	$HI = -42.379 + 2.04901523T + 10.14333127RH - 0.22475541TRH - 0.006837837T^2 - 0.05481717RH^2 + 0.001228747T^2\mathrm{RH} + 0.00085282TRH^2 - 0.00000199T^2\mathrm{RH}^2$	Rothfusz, 1990 (in his eqn (2)
HUMIDEX	T, e	$H = T + (0.5555 \times (e - 10.0))$	Masterton and Richardson, 1979 (in eqn (3)
Wet-bulb globe temperature (WBGT)	T_{nwb}, T_g, T	$\mathrm{WBGT} = 0.7T_{nwb} + 0.2T_g + 0.1T$	Yaglou and Minard, 1957 (in eqn (4)
Simplified WBGT (W)	T, e	$W = 0.567T + 0.393e + 3.94$	ABOM, ACSM, 1984 (in his eqn (5)
Environmental stress index (ESI)	T, RH, SR	$\mathrm{ESI} = 0.63T - 0.03RH + 0.002SR + 0.0054(T \times RH) - 0.073(0.1 + \mathrm{SR})^{-1}$	Moran *et al*., 2001 (in eqn (6)

military, civil engineers, sports associations (especially Australian), and the Australian Bureau of Meteorology. Despite its development from a narrow demography (fit military males in full battle dress), it has been assessed to have some applicability, worldwide, within limits (Parsons, 2006). It is the only heat index to have known thresholds relating directly to levels of physical activity (Tables II and III). However, it requires non-standard input variables – a black globe temperature equilibrated over 30 min and an exposed wet-bulb temperature, to take into account the effect of direct heating from the sun, and evaporative cooling due to wind which are excluded from traditional wet- and dry-bulb measurements. Very few formal measurements of WBGT exist. Normal practice is to use either a handheld field device that gives an approximation or a model to predict it based on standard meteorological quantities. Unfortunately, to do this properly requires short-wave and long-wave actinic fluxes which are also not available with sufficient coverage for this study. Therefore, we use the 'simplified WBGT' (hereafter denoted simply as 'W'), developed by the Australian Bureau of Meteorology (ACSM, 1984), which depends only on temperature and humidity and represents heat stress for average daytime conditions outdoors. It assumes moderately high radiation levels and light wind conditions. This can result in a slight overestimation of heat stress in cloudy or windy conditions and during night-time and early morning but underestimation during periods of full sun and light winds.

By using this equation we are neglecting the impact of wind or cloudiness on heat stress. We do not expect changes to radiation or windiness to have a significant systematic impact globally on trends in W. Consensus cloud-cover changes simulated by GCMs are typically no more than 2% °C^{-1} regionally (Meehl *et al*., 2007), yielding insolation changes of a few percent per °C which would have a negligible effect on heat index trends. Neglecting this impact, however, will produce large errors for individual days, and may be important for regional changes in locations where weather patterns change significantly as climate warms. An interesting regional phenomenon is the stilling of winds in

Table II. Military thresholds of WBGT. (*Source: USARIEM*).

W	Description	Level of Risk
26	Caution over extremely intense physical exertion	Moderate
28	Possible reduction in heavy exercise for non-acclimatised	High
29	Suspension of strenuous exercise for non-acclimatised	–
31	Limited activity for acclimatised	–
32	Suspension of physical training and strenuous exercise for all (excluding essential operational commitments not for training purposes)	Extreme

Table III. Recommended work/rest thresholds for fit military personnel in full battle dress. (*Source: ACGIH, 1996*).

Work/Rest ratio for 1 hour (%)	Work load and *WBGT* threshold (°C)		
	Light	Moderate	Heavy
100/0	30.0	26.7	25.0
75/25	30.6	28.0	25.9
50/50	31.4	29.4	27.9
25/75	32.2	31.1	30.0

Australia, likely due to pole-ward migration of the mid-latitude jet (McVicar *et al*., 2008). If all of this trend (1 ms^{-1} $century^{-1}$) were due to warming it would equate to roughly 1 ms^{-1} $^{\circ}C^{-1}$, though this is 3–4 times the model-predicted equilibrium value at that latitude (Kushner *et al*., 2001) so it may not all be due to warming. Even if it were, it would equate to only about half the direct effect of a decrease in temperature based on Hunter and Minyard's (1999) approximation of WBGT.

Although WBGT and other heat indices are designed to resemble temperatures, they should be thought of as relative measures of heat: a higher value should, for a typical person, correspond to greater thermal load and higher chance of heat stress. To make any absolute interpretation of such variables requires empirically established thresholds of heat-related impacts or limitations to activity. The WBGT was originally designed by the US military as a measure to prevent heat-related injuries during training. As such, associated thresholds are not wholly applicable to the general population but should be applicable to fit, healthy, adults. The WBGT thresholds for this study are 28, 32, and 35 °C and refer to high, very high, and extreme risk to health, respectively, for people undertaking physical activity. At 32 °C, cancellation of major sporting events is considered such as the Australian Open (Leighton and Baldwin, 2008). The highest threshold, 35 °C, is approximately equal to skin temperature and therefore seen as a critical level at which it is advisable to cease all physical activity.

2.2. Data sources and calculation of W

The quality-controlled and homogenised surface humidity dataset HadCRUH (W08) is used (obtainable in gridded monthly mean anomaly form from www.hadobs.org). The authors follow a similar procedure to create a homogenised pentad (five-day mean) W dataset. While efforts begin with hourly station data, homogenisation is applied at pentadal resolution. Ideally, data would be homogenised at the daily or even sub-daily time scale since instrument errors can, in principle, vary throughout the day. To the authors' knowledge however there is no near-global dataset fitting this criterion at present, although one is under development at the UK Met Office.

The quality-controlled hourly station source data, initially provided by the Integrated Surface Dataset (ISD) from the National Climatic Data Center (NCDC) (Lott *et al*., 2001), are available as dewpoint temperature T_D and dry-bulb temperature T. Hourly vapour pressure e is calculated using an equation from Buck (1981):

$$
\begin{aligned}
e_s &= 6.1121 \times f \times \mathrm{EXP}(((18.729 \\
&\quad - (T/227.3))T)/(257.87 + T)) \qquad (7)\\
f &= 1.0007 + (0.00000346 \times P)\\
&\quad \text{(actually using}\\
&\quad P = 1013,\ \text{so}\ f = 1.004)
\end{aligned}
$$

$$
\begin{aligned}
P &= 1013 - (Z/10)\\
Z &= \text{elevation from ISD station data}
\end{aligned}
$$

Equation 5 (Table I) is then used to calculated hourly W. The data have undergone quality control both at NCDC and as part of the HadCRUH processing (W08).

The station hourly W and T data are processed to give pentad mean $\overline{W}$ and $\overline{T}$, pentad mean of the daily maxima $\overline{W}_m$ and $\overline{T}_m$, and pentad overall maximum (maximum hourly value within the pentad) W_{mm} and T_{mm}. Hereafter, these variables will be referred to collectively as W_{vars} and T_{vars}. While $\overline{W}_m$ dampens the actual extremes by averaging maxima over the pentad, it is useful for representing *extended periods* of high heat which have been shown to be linked to classical heat stress and heat-related mortality in the very old, very young, and those with ill health. By contrast, W_{mm} is a *single extreme event* indicator more relevant to short-term (but possibly frequent) impacts on daytime activities by healthy individuals (exertional and occupational heat stress).

HadCRUH was homogenised semi-manually at pentad mean resolution with breakpoints identified for specific humidity q also applied to relative humidity, *RH*. This assumes that there are no additional inhomogeneities in temperature – a reasonable assumption where inhomogeneities arise from station/instrument moves. This is not a perfect solution, but sufficient, considering available time and lack of metadata. A comparison of homogenised and non-homogenised q trends from HadCRUH reveals slightly smaller trends in the latter for the Globe and Northern Hemisphere but slightly larger trends in the Tropics all of the order of 0.01 g kg^{-1} per decade. So, as the W_{vars} and T_{vars} are created from hourly unhomogenised data, homogeneity adjustments are necessary.

For physical consistency with HadCRUH, breakpoint dates identified for each HadCRUH station pentad mean q are used for homogenisation of the W_{vars} and T_{vars}. A set of neighbour stations is required for each station. These are chosen based on correlation strength with the target station for the given variable. For W_{vars} the HadCRUH q neighbour lists are used, since the spatial decorrelation length scale of W is dominated by that of q. For T_{vars} a set of temperature-specific neighbour lists are created following the same method (W08). As for HadCRUH, adjustments are made to all data preceding each breakpoint based on the difference in the median of the candidate minus neighbour difference series before and after. There are two iterations of adjustments, to allow for removal of some discontinuities that are masked by other larger ones. For the second iteration. a new neighbour composite and difference series is created using the adjusted data.

Adjustment amount and frequency for $\overline{W}$ and $\overline{T}$ at all stations used in this study are shown in Figure 1. Adjustments are distributed almost evenly around zero

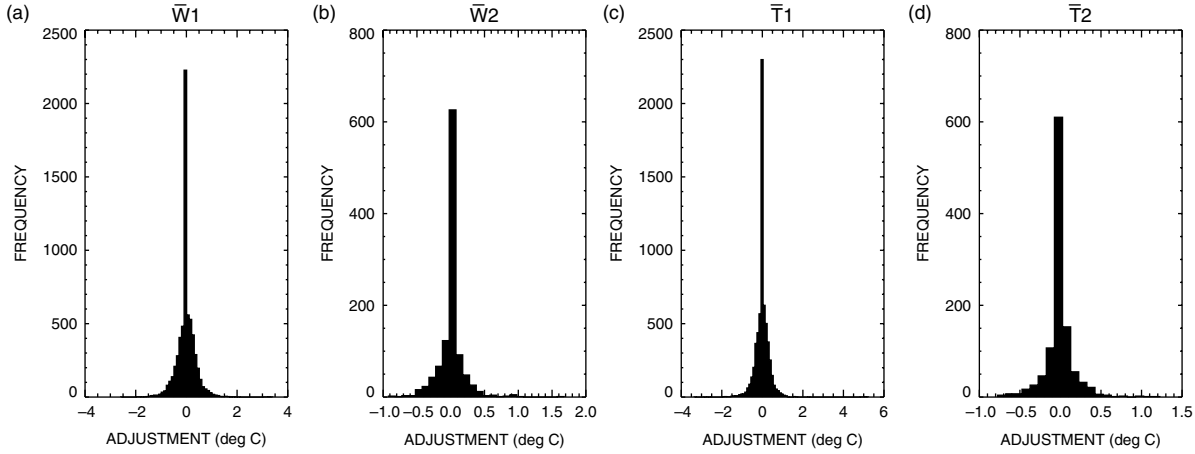

Figure 1. Frequency distributions of adjustment quantities made to all stations for pentad $\overline{W}$ a) and b) and pentad $\overline{T}$ c) and d) over two iterations of the homogenisation process. Adjustment histograms are similar for the other statistics (pentad $\overline{W}_m$, pentad $\overline{T}_m$, pentad W_{mm}, and pentad T_{mm}) (not shown).

for all variables and all iterations. There are 29 stations identified as requiring large adjustments up to nearly 4 °C, e.g. station 535880 (Wutai Shan, China) has a very large ~3.5 °C inhomogeneity towards the end of the record. Similar to q in HadCRUH, homogenisation has the effect of increasing global and Northern Hemisphere W_{vars} trends by 0.01 °C per decade or less. There is no attempt to remove non-abrupt inhomogeneities (Elliott, 1995). Notably, urban warming has a real effect on humans and, therefore, should not be removed. Due to lack of true urban stations however, the real urban climate is very poorly represented by observational records. Given the greater intensity of heat stress due to likely higher radiative impact and inhibited night-time cooling (Grimmond, 2007) this study should probably be considered conservative and likely an underestimate in terms of urban environments.

This study explores summertime data only, with results aggregated over 15 regions. Summer is defined as: June, July, and August (JJA) for the US and European regions; December, January, and February (DJF) for the Australian regions; and April, May, June, July, August, and September (AMJJAS) for the Caribbean, India, and eastern China. In calculating region means, stations above 1000 m elevation are omitted. This is due to issues of inconsistency when averaging over very different climates; high altitudes are highly unlikely to experience hazardous high extremes of temperatures. Thus, results are representative only of the portion of each indicated region below this altitude. Regions used are described in Table IV.

A 17-strong ensemble of HadCM3 historical and A1B Scenario runs of daily T and RH from the QUMP (Quantifying Uncertainty in Model Prediction) archive (Collins *et al.*, 2010) are used. These cover a range of perturbations of the GCM to give some measure of uncertainty. They are used to produce regional changes relative to 1974–2003 in summertime mean T, RH, and W (calculated from Equations 7, 8, and 9) for the 2020s (2005–2034) and 2050s (2035–2064). This provides some insight into the likelihood of specific W increases in each region and the validity of assumptions made in creation of the W_{vars} exceedance model.

3. W mean state, threshold exceedance and trends over recent decades

W is an unfamiliar quantity to many. While W values are similar to T, they are usually lower, especially in cloudy low humidity conditions, although they can be higher with sufficient radiative heating and high humidity. Global summertime distributions are similar to that of T and q: they are highest in the Tropics and decrease pole-wards. Figure 2 shows summertime zonal means of pentad $\overline{W}$, pentad $\overline{W}_m$, and pentad W_{mm} and a map of summertime means for W_{mm}. There is little difference between the zonal distributions of the three variables. The highest values lie in the summer hemisphere deep to sub-tropics where values in excess of 30 °C are common. Of the grid-boxes with data present, the most extreme values occur over the hot and dry regions. The Tropics are more consistently hot and humid but rarely see such extreme values.

Note that W is a heat index only and gives no useful information for values below 15 °C. There is a degree of acclimatisation for residents of high W regions whereby prolonged exposure to high heat results in improved sweating efficiency (Taylor, 2006). For short-term visitors to high W regions (military personnel, athletes, holiday makers, etc.), lack of acclimatisation combined with high W poses strong health risks. Current percentage exceedances of summertime pentad W_{mm} and $\overline{W}_m$ of the three thresholds for each region are quantified in Figure 3 (W_{mm} only) and Tables V and VI. Exceedance of the 28 °C threshold in both W_{mm} and $\overline{W}_m$ is common to all regions although still rare (at <5% and <1% of summertime pentads, respectively) for the UK. These exceedances are close to 100% for southeast USA, northern Australia, all of India, and the

Table IV. Summary of study regions.

Region	Latitude boundaries	Longitude boundaries	Number of stations
Northwestern USA	40 °N–50 °N	125 °W–100 °W	24
Northeastern USA	40 °N–50 °N	100 °W–70 °W	64
Southwestern USA	30 °N–40 °N	125 °W–100 °W	5
Southeastern USA	30 °N–40 °N	100 °W–70 °W	25
UK	50 °N–60 °N	5 °W–5 °E	86
France	40 °N–50 °N	0 °E–10 °E	103
Northwestern Australia	10 °S–25 °S	115 °E–135 °E	10
Northeastern Australia	10 °S–25 °S	135 °E–155 °E	17
Southwestern Australia	25 °S–40 °S	115 °E–135 °E	5
Southeastern Australia	25 °S–40 °S	135 °E–155 °E	23
Caribbean	10 °N–25 °N	85 °W–60 °W	32
Northern India	15 °N–25 °N	70 °E–90 °E	21
Southern India	5 °N–15 °N	70 °E–90 °E	12
Northeastern China	30 °N–40 °N	105 °E–125 °E	82
Southeastern China	20 °N–30 °N	105 °E–125 °E	94

Caribbean. All regions except the UK currently experience both single events and extended periods above the 32 °C threshold, this is highest in the Caribbean. There is currently low exceedance of the extreme 35 °C threshold although this occurs for more than 10% of the summertime for the moist tropical regions of southeast China, northwest Australia, the Caribbean, and India.

Recent trends in percentages of summertime threshold exceedance are shown in Figure 4 (W_{mm} only) and Tables V and VI for W_{mm} and $\overline{W}_m$, respectively. In general, frequency of single exteme event (W_{mm}) threshold exceedance has increased more than that for extended periods of heat ($\overline{W}_m$) threshold exceedance for dryer regions. The opposite is true for very moist regions. In total, ~86% of all trends and all regions are positive and ~50% are significant ($\leq$10% level). Only trends for northeast USA $\overline{W}_m$ are negative (two are significant). The Australian region as a whole gives a less coherent picture in terms of significantly increasing W.

Regions experiencing current exceedance rates near zero, or 100% for a given threshold, will obviously show small or no trends for that threshold. As a result, higher W regions (climatologically) show greater trends for the highest thresholds while lower W regions such as the UK and France show larger trends for the lower thresholds. France, a region with relatively moderate climatological W, shows the greatest trends in the 28 °C threshold exceedance at 6.56 and 3.15% 10 yr^{-1} for W_{mm} and $\overline{W}_m$, respectively. This result is likely influenced, in part, by extremes in 2003 as discussed later. For the 32 °C threshold, trends are largest (significant at 5%) in northern India at 3.21 and 4.45% 10 yr^{-1} for W_{mm} and $\overline{W}_m$, respectively. For the extreme threshold of 35 °C, the largest trends (significant at 5%) are found in the Caribbean at 6.71 and 4.80% 10 yr^{-1} for W_{mm} and $\overline{W}_m$, respectively. Notably India and the Caribbean, hot and humid regions already experiencing high W, show large and significant increases.

4. A simple statistical model for predicting threshold exceedance

To quantify likely future summertime exceedances of W thresholds should warming continue, a simple statistical model is proposed and tested. The basic assumption of the model is that the frequency distribution of summertime W will shift uniformly, with no significant systematic changes in shape (e.g. skewness, variance, or kurtosis). To predict the change in mean W per °C change in mean T, it is further assumed that mean RH remains constant, and resulting changes are considered as a function of warming amount.

While the main test of these model assumptions will be to see how well it predicts observed exceedances, the annual summertime variance in W_{vars} is examined to seek significant trends over time. The assumption of stationary variance is found to be consistent with the data in most, though not all regions (Table VII). About 22% of the time series show significant trends at the 5% level, most of them positive, which suggests a field-significant overall trend toward higher variance; the largest trends however, in the SW USA region, are negative at -0.27 and -0.30 °C for $\overline{W}_m$ and W_{mm}, respectively. Thus, it is not clear whether the significant regional trends are part of an overall global trend. One caveat is that individual stations are often missing over portions of the time series, which will contaminate trend estimates. Also, it should be noted that trends in variance do not automatically imply a changing relationship between high W extremes and the mean W, as they could result solely from changes to extremes at the low (mild) end of the range. It is therefore concluded that this assumption of stationary variance will not affect general patterns in the results, but may over- or underestimate results in specific regions. Our interpretation of the regional variance trends is therefore that, while distributions about the mean will likely vary somewhat especially regionally and on decadal time scales, subsequent tests based directly on high extremes

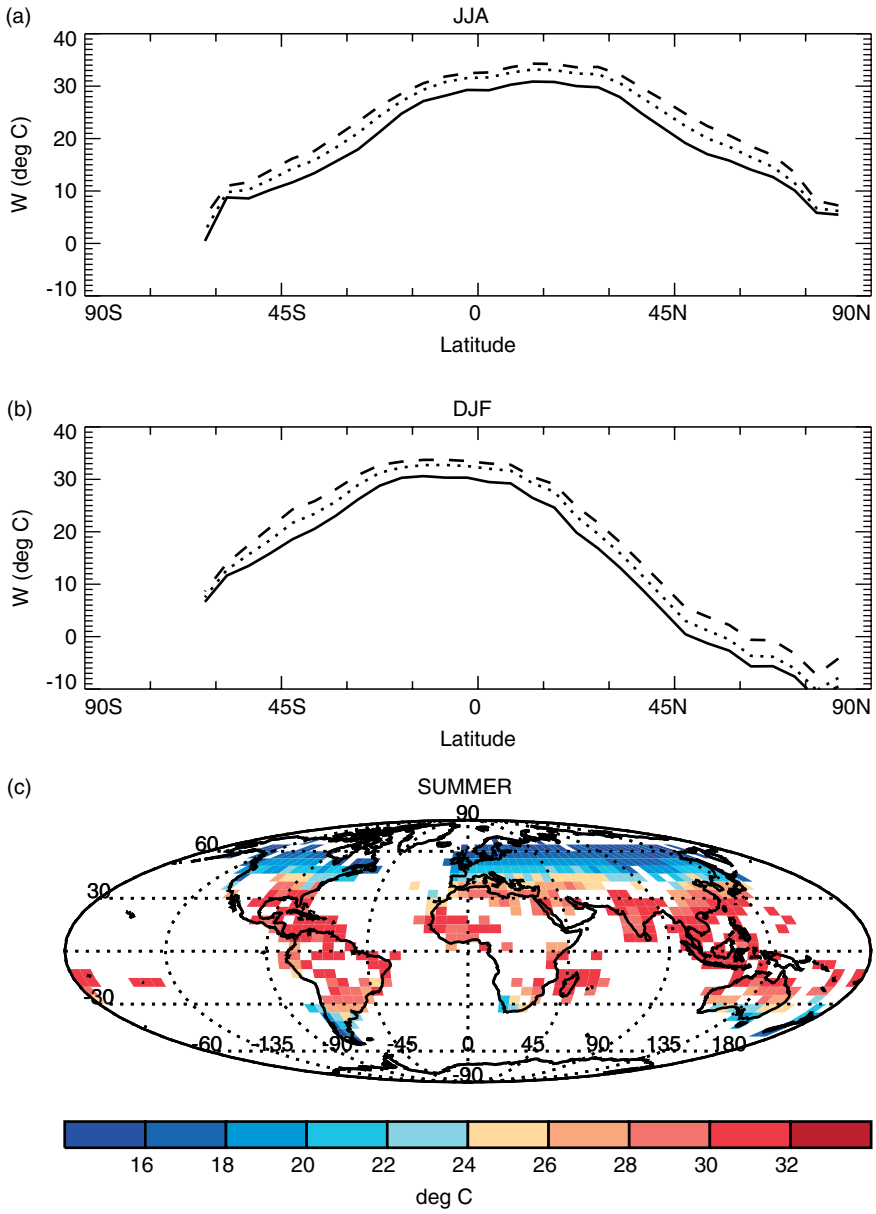

Figure 2. Climatological W for the globe in °C. Panels a) and b) show zonally averaged June, July, and August (JJA), and December, January, and February (DJF) means, respectively, for pentad $\overline{W}$ (solid line), pentad $\overline{W}_m$ (dotted line) and pentad W_{mm} (dashed line). Panel c) shows hemispheric summer (Northern Hemisphere JJA and Southern Hemisphere DJF) mean pentad W_{mm}.

are more appropriate for assessing the applicability of our model to such extremes.

To specify the model, for all W_{vars}, summertime pentads in a region are accumulated, detrended, and subtracted from the respective station summertime climatology. This yields a sample distribution of anomalies that can then be added to any mean W_{vars} to obtain a shifted distribution, from which the exceedance of the three thresholds is calculated. To test the model, an annual time series of exceedances is predicted for all W_{vars} and regions based on the observed sequence of summertime means.

The prediction model successfully reproduces most of the inter-annual variability in exceedance rates: the vast majority of W_{vars}/region combinations give a strong positive correlation (>0.6) of observed with predicted exceedance time series (88% for $\overline{W}_m$ and 89% for W_{mm} of all regions and thresholds). Northwest USA is an exception, consistently correlating poorly. RMS errors range from 1.6 to 2.5% exceedance over all W_{vars} and thresholds. Trends are also well predicted, with correlations between predicted and observed linear trends among regions of 0.6 or higher for all W_{vars} and thresholds (Figure 4, Tables V and VI). RMS errors range from 0.11 to 0.97% exceedance. The relationship is indistinguishable from linear and has a slope close to unity. The model captures the key regional variations in trends, including the strong and significant trends in France, the Caribbean, and India, and negative trends for northeast USA. It does overestimate trends for southwest USA in both $\overline{W}_m$ and W_{mm}, but in each case the sign of the predicted trend is correct. There are less than 5%

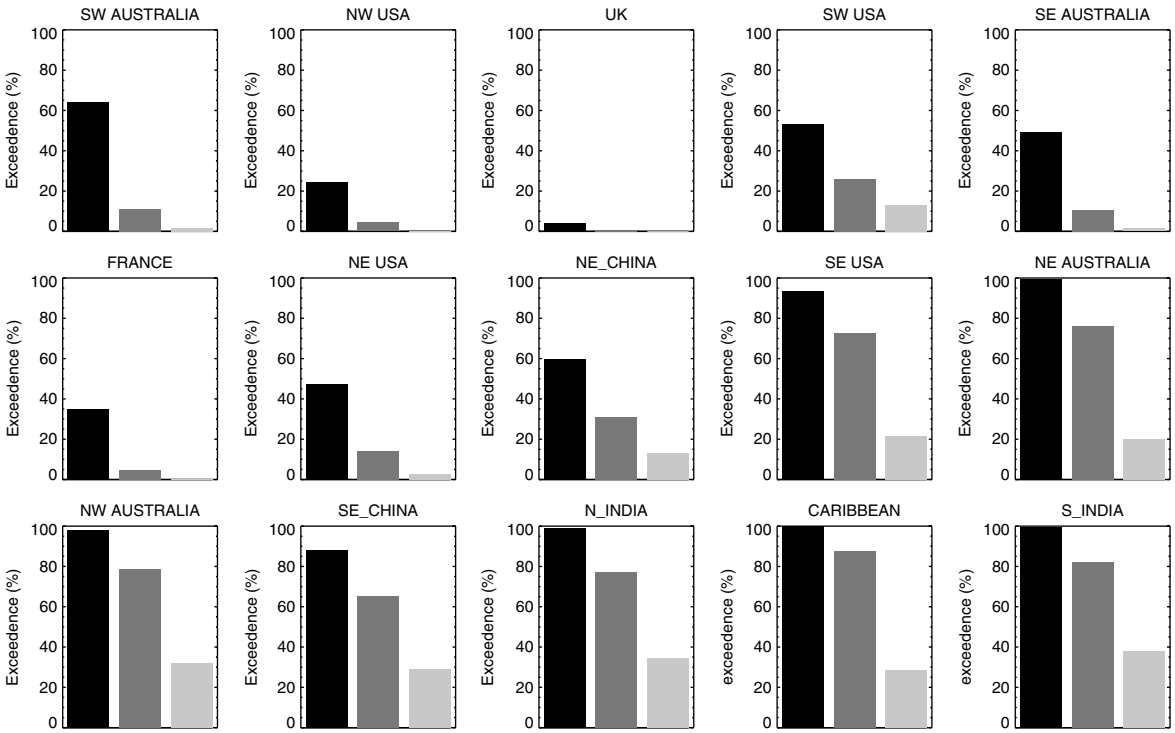

Figure 3. Present (1973–2003) summertime W_{mm} exceedance of the 28 °C (black), 32 °C (dark grey) and 35 °C (light grey) thresholds for 15 regions. Exceedance is quantified as a percentage of summertime pentads. Summertime is quantified as June to August for USA and European regions, December to February for Australian regions, and April to September for China, India, and the Caribbean. Southwestern Australia, northwestern USA, UK, southwestern USA and southeastern Australia (top row) are 'dry' regions where regional mean summertime specific humidity is less than 10 g kg^{-1}. France, northeastern USA, northeastern China and southeastern USA (mostly middle row) are 'moderate' regions where regional mean summertime specific humidity is between 10 and 15 g kg^{-1}. Northeastern Australia, northwestern Australia, southeastern China, northern India, the Caribbean, and southern India (mostly bottom row) are 'moist' regions where regional mean summertime specific humidity is greater than 15 g kg^{-1}.

of cases where the prediction model trend exceeds the two-sigma uncertainty of the actual sample exceedance trend.

To test the prediction model more rigourously, the significance of discrepancy between each modelled and actual trend is computed, based on the uncertainty of linear fit to the time series of annual prediction model data differences. Discrepancies greater than two sigma-(95% significance) significance are found for 19 out of a total of 128 region/W_{vars}/threshold combinations (most of these for the 32 °C threshold). Approximately seven significant discrepancies (5%) only are expected by chance if the model is perfect; thus, there is evidence that in some regions the assumptions of the model are not completely valid, indicating statistically significant trends in the breadth or shape of the regional W distribution. One example where this is not unexpected is France, due to the extreme 2003 event. Since the discrepancies over this time period are all smaller than the absolute trend uncertainty, however, and show no systematic character, it is not clear whether they are representative of longer-term trends (i.e. physically significant) or just decadal variations in distribution breadth. In any case, the model captures most of the changes including trends, and it is concluded that there is no justification to add further complexity at this time.

Figure 4 clearly shows that for the 32 and 35 °C, the largest trends are in the most moist regions, while for the 28 °C threshold, they are not. This is largely because mean W is highly correlated to mean q, and exceedance trends are highest for intermediate exceedance rates as discussed earlier. However, it is shown below that for more moist climates, a given warming leads to larger changes in W, which presumably, also contributes to the prevalence of high exceedance trends in the most humid regions.

5. Future exceedances under a warming climate

5.1. Exceedance for a given rise in region mean temperature assuming constant relative humidity

Four future climates are investigated here, with regional mean warmings (in T) of 1, 2, 3, and 5 °C applied to all W_{vars}. This is to decouple the questions of how much warming will happen and how much heat will be increased by a given warming. To predict the likely resulting shift in W_{vars}, a region-specific shift is calculated based on the climatological RH and W_{vars} for that region, for each change in T, based on the constant-RH assumption. This assumption is upheld for the most part in both GCM and observed studies over large scales (Allen and Ingram, 2002; W08) although

Table V. Observed summertime threshold exceedance and trends and predicted threshold exceedance trends for $\overline{W}_m$ for 15 regions over the period 1973–2003. Exceedance is shown as a mean percentage of summertime pentads exceeding each threshold. The trends refer to a percentage increase per decade in percentage of summertime pentads exceeding each threshold and significance is denoted as [a] and [b] for 5 and 10%, respectively. Trends are fitted using least squares regression. Data are first pre-whitened assuming good fit to an AR1 noise process and allowing for autocorrelation (Cochrane and Orcutt, 1949; Wei, 1990). Significance of trends relative to time series variability is tested using a two-tailed t-test. Correlations show the observed verses predicted percentage exceedance time series for each threshold for $\overline{W}_m$ pentads. Regions are listed in order of summertime mean specific humidity and grouped such that light grey = <10 g kg^{-1}, white = 10–15 g kg^{-1} and dark grey = >15 g kg^{-1}.

Region	28 °C Threshold				32 °C Threshold				35 °C Threshold			
	Exceedance	Observed trend	Predicted trend	Correlation	Exceedance	Observed trend	Predicted trend	Correlation	Exceedance	Observed trend	Predicted trend	Correlation
S-W Australia	29.95	1.63	1.20	0.95	1.29	0.75[a]	0.17	0.63	0.00			
N-W USA	10.12	0.67[b]	1.34[a]	0.66	0.88	0.25[b]	0.25[a]	0.16	0.01	0.02[b]	0.01[a]	−0.14
UK	0.32	0.10	0.08	0.83	0.00				0.00			
S-W USA	39.20	1.61	3.66[a]	0.89	17.23	−0.05	2.19[a]	0.61	6.82	1.15[b]	1.73[a]	0.77
S-E Australia	24.25	0.76	0.45	0.88	2.38	0.29	0.10	0.68	0.09	−0.02	0.01	0.59
France	14.69	3.15[a]	3.18[a]	0.94	0.89	0.43[a]	0.54[a]	0.88	0.03	0.02	0.04[b]	0.63
N-E USA	21.49	−1.67	−1.05	0.93	3.21	−0.63[b]	−0.32	0.69	0.23	−0.10[b]	−0.05	0.30
N-E China	43.10	1.70[a]	1.57[a]	0.85	16.98	0.70	1.14[a]	0.81	4.39	0.59[b]	0.65[a]	0.70
S-E USA	84.35	0.33	0.70	0.85	47.41	1.87	2.02	0.92	4.64	1.03[b]	0.47	0.73
N-E Australia	97.66	−0.42	0.06	0.64	50.74	0.71	0.32	0.97	5.34	0.79	0.01	0.76
N-W Australia	94.26	0.72	0.36[b]	0.64	62.94	0.84	1.79[b]	0.86	13.95	1.22	1.46[b]	0.77
S-E China	75.32	0.92[b]	0.70[a]	0.95	48.21	0.19	1.11[a]	0.76	10.08	1.50[a]	1.52[a]	0.70
N India	96.93	1.07[a]	1.00[a]	0.93	61.41	4.45[a]	4.25[a]	0.99	17.16	3.64[a]	3.60[a]	0.97
Caribbean	99.17	0.35[a]	0.28[a]	0.49	76.85	3.92[a]	4.73[a]	0.96	12.33	4.80[a]	3.77[a]	0.95
S India	97.10	0.61[a]	0.77[a]	0.80	70.01	3.71[a]	3.45[a]	0.96	18.01	3.84[a]	3.61[a]	0.97

[a] 5% threshold and significance.
[b] 10% threshold and significance.

Table VI. Observed summertime threshold exceedance and trends and predicted threshold exceedance trends for W_{mm} for 15 regions over the period 1973–2003. Exceedance is shown as a mean percentage of summertime pentads exceeding each threshold. The trends refer to a percentage increase per decade in percentage of summertime pentads exceeding each threshold and significance is denoted as [a] and [b] for 5 and 10% respectively. Trends are fitted using least squares regression. Data are first pre-whitened assuming good fit to an AR1 noise process and allowing for autocorrelation (Cochrane and Orcutt, 1949; Wei, 1990). Significance of trends relative to time series variability is tested using a two-tailed t-test. Correlations show the observed *versus* predicted percentage exceedance time series for each threshold forW_{mm} pentads. Regions are listed in order of summertime mean specific humidity and grouped such that light grey = <10 g kg^{-1}, white = 10–15 g kg^{-1} and dark grey = >15 g kg^{-1}.

Region	28 °C Threshold				32 °C Threshold				35 °C Threshold			
	Exceedance	Observed trend	Predicted trend	Correlation	Exceedance	Observed trend	Predicted trend	Correlation	Exceedance	Observed trend	Predicted trend	Correlation
S-W Australia	64.20	2.01	2.48	0.92	11.26	3.68[a]	2.10[a]	0.89	1.54	0.61[a]	0.25[a]	0.64
N-W USA	24.29	2.35[a]	2.89[a]	0.87	4.42	0.54[b]	0.89[a]	0.45	0.36	0.10	0.12[a]	−0.06
UK	4.28	1.04[b]	0.58	0.89	0.11	0.10[a]	0.03	0.60	0.00	–	–	–
S-W USA	53.27	3.67	4.13[a]	0.90	26.11	0.52	3.53[a]	0.63	12.94	0.92	2.38[a]	0.68
S-E Australia	49.50	1.25	1.29	0.97	10.80	1.11	0.75	0.84	1.41	0.20	0.16	0.67
France	34.90	6.56[a]	5.34[a]	0.96	4.48	1.48[a]	1.75[a]	0.89	0.28	0.13[a]	0.21[a]	0.74
N-E USA	47.62	−1.32	−1.54	0.97	14.28	−1.64	−0.91	0.89	2.77	−0.61[b]	−0.32	0.70
N-E China	59.66	1.72[a]	1.44[a]	0.78	30.99	1.68[a]	1.45[a]	0.84	12.91	0.64	1.09[a]	0.78
S-E USA	93.72	−0.19	0.38	0.78	72.47	0.87	1.43	0.90	21.62	2.90	1.53	0.85
N-E Australia	99.38	−0.23	0.08	0.47	75.97	−0.06	1.36	0.94	20.32	2.66[a]	1.06	0.89
N-W Australia	98.00	0.51	0.12	0.61	78.58	1.64	1.39[b]	0.86	32.13	0.68	1.70	0.78
S-E China	87.86	0.84	0.28	0.85	65.49	0.25	0.63	0.87	29.00	0.93	1.29	0.74
N India	99.00	0.48[a]	0.38[a]	0.81	77.03	3.21[a]	3.12[a]	0.96	34.43	3.96[a]	3.73[a]	0.98
Caribbean	99.80	0.09[a]	0.07[a]	0.29	87.68	2.02[a]	2.93[a]	0.91	28.31	6.71[a]	5.90[a]	0.98
S India	99.50	0.14[b]	0.20[a]	0.35	82.21	1.68[a]	1.49[a]	0.88	37.72	3.26[a]	2.89[a]	0.97

[a] 5% threshold and significance.
[b] 10% threshold and significance.

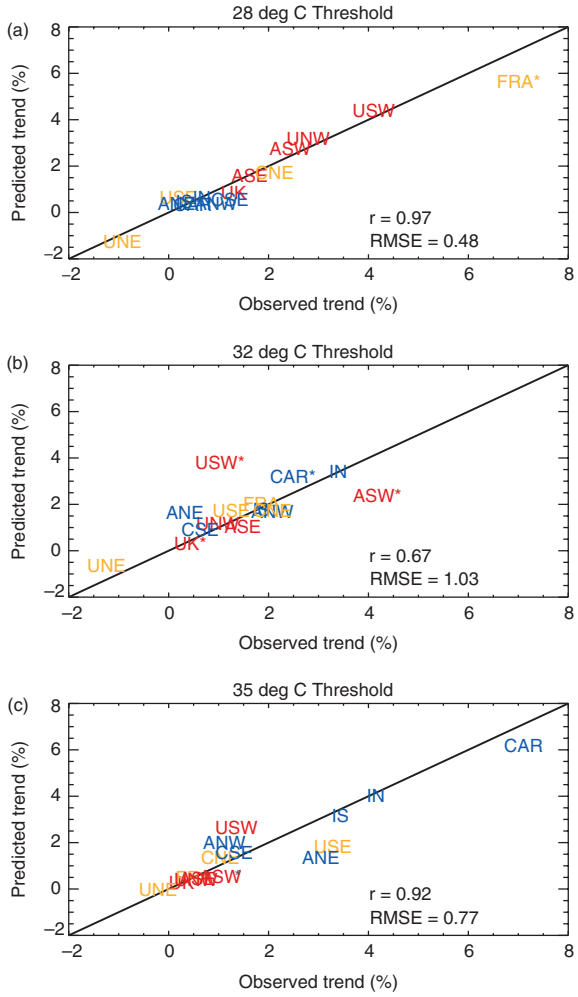

Figure 4. Comparison of predicted and observed trends in summertime pentad W_{mm} exceedance for each threshold and region over the 1973–2003 period colour coded by climatological (1974–2003) summertime specific humidity [red = <10 g kg^{-1}, yellow = 10–15 g kg^{-1}, blue = >15 g kg^{-1}]. The predicted-observed difference series are considered significantly different (at 5%) if a significant linear trend is found; these regions/thresholds are identified by an asterisk. Correlation r values for all regions predicted verses observed trends in each threshold are shown in the bottom right hand corner. Predicted minus observed RMS difference in exceedances across all thresholds combined is 0.79%. To aid clarity, region names have been abbreviated as follows: UK = United Kingdom; FRA = France; UNW = Northwestern USA; UNE = Northeastern USA; USW = Southwestern USA; USE = Southeastern USA; ANW = Northwestern Australia; ANE = Northeastern Australia; ASE = Southeastern Australia; ASW = Southwestern Australia; IN = Northern India; IS = Southern India; CNE = Northeastern China; CSE = Southeastern China; and CAR = the Caribbean.

small changes over recent years over land, at least, have been detected (Simmons *et al.*, 2010), and significant trends may be expected in certain regions or latitude bands owing to shifting circulation patterns. Calculation at such coarse resolution is not ideal and will lead to a small underestimate of the change in humidity but it was the only viable option due to data availability at the time of analysis.

The cosine-latitude-weighted mean summertime T_{vars} and W_{vars} are calculated over the climatological period

Table VII. Trends in variability (standard deviation) of the annual summertime W for each region and variable. Trends are fitted and significance tested as described in Table V where [a]** and [b]* show significance at the 5 and 10% levels, respectively.

Region	$\overline{W}_m$	W_{mm}	$\overline{W}$
N-E Australia	0.11[a]	0.09[b]	0.17[a]
N-W Australia	−0.05	−0.09[b]	−0.02
S-E Australia	0.05	0.03	0.15[a]
S-W Australia	0.13[a]	0.12[a]	0.11[a]
Caribbean	0.05[a]	0.05[a]	0.02
N-E China	−0.01	−0.02	−0.02
S-E China	−0.03	−0.03	−0.04
France	0.05	0.06	0.05
N India	0.01	−0.02	0.01
S India	0.04[a]	−0.01	0.06[a]
UK	0.08	0.13[b]	0.08
N-E USA	−0.07	−0.06	0.01
N-W USA	−0.06	−0.05	−0.02
S-E USA	0.10[b]	0.11[b]	0.09
S-W USA	−0.27[b]	−0.30[b]	−0.19

[a] 5% threshold and significance.
[b] 10% threshold and significance.

(1974–2003) using data from each station within the region. Region mean vapour pressure e is calculated from all T_{vars} with equivalent W_{vars} using a rearrangement of Equation 5 (Table I).

$$e = (W - 3.94 - 0.567\ T)/0.393 \tag{8}$$

The region mean summertime saturated vapour pressure (e_s) is calculated from region mean T_{vars} using Equation 7. The region mean summertime RH for all quantities is calculated from e and e_s.

$$RH = (e/e_s) \times 100 \tag{9}$$

New region mean T_{vars} for each increment is calculated by adding the 1, 2, 3, and 5 °C. From this, a new region mean e_s (all variables) is calculated using equation 7 assuming no/negligible change in P over time. A new e (all variables) is then calculated using RH, and the new e_s by rearranging Equation 9. The new region mean W_{vars} are then calculated from new e and new T for each warming increment and variable using equation 5 (Table I). The model anomaly distribution is then added to each of the incrementally higher region W_{vars} means and threshold exceedance calculated. Results for $\overline{W}_m$ and W_{mm} are shown in Figure 5.

Clearly, a warming climate brings more frequent W_{vars} extremes in all regions, but the rate of increase varies regionally. This strongly depends on how close to 0 or 100% the current exceedance rate is, as discussed in Section 3. It also depends on the shape of the distribution for each region. A comparison of northeast China and southwest Australia demonstrates this where summertime 28 °C exceedance in pentad W_{mm} is comparable (60 and 64%, respectively), but for the 32 and 35 °C thresholds,

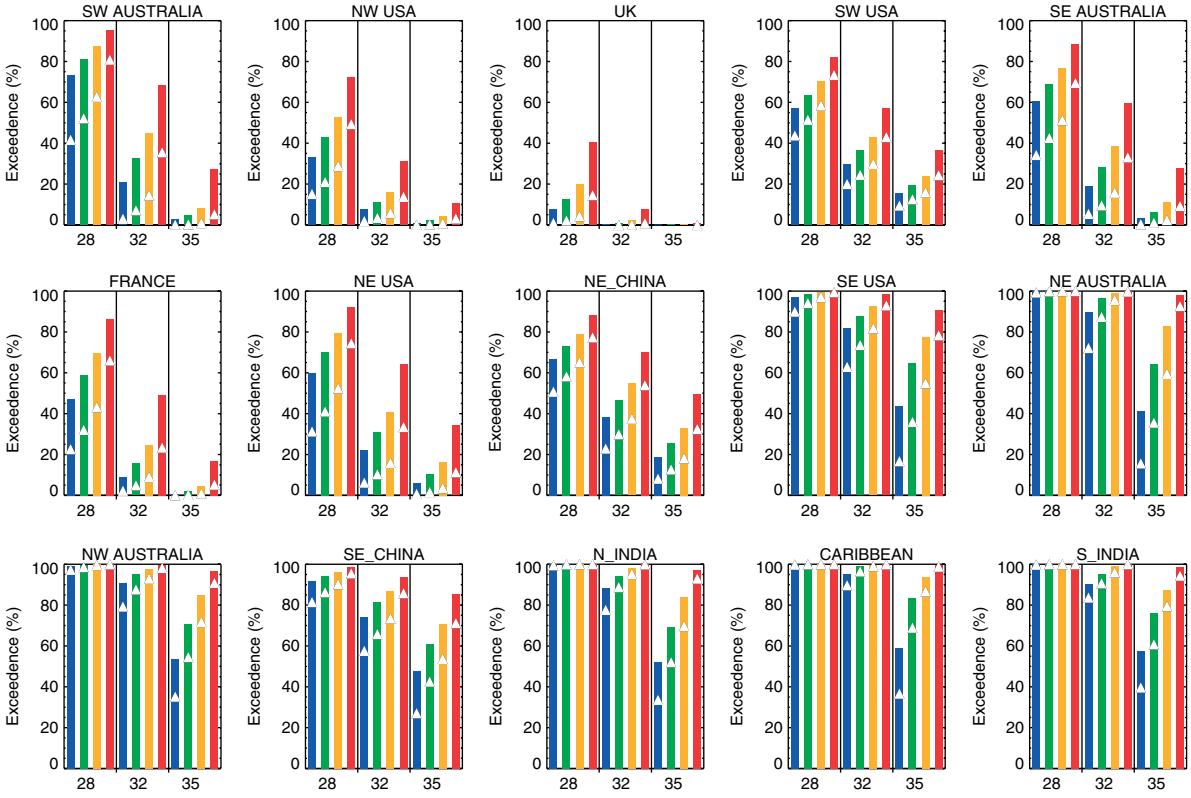

Figure 5. Summertime threshold exceedance for both pentad W_{mm} (coloured bars) and $\overline{W}_m$ (triangles) predicted for a warming climate for 15 regions. Predicted threshold exceedance is shown for 28, 32, and 35 °C under a 1 °C (blue), 2 °C (green), 3 °C (yellow) and 5 °C (red) warming in regional temperature while holding relative humidity constant. Southwestern Australia, northwestern USA, UK, southwestern USA, and southeastern Australia (top row) are 'dry' regions where regional mean summertime specific humidity is less than 10 g kg^{-1}. France, northeastern USA, northeastern China, and southeastern USA (mostly middle row) are 'moderate' regions where regional mean summertime specific humidity is between 10 and 15 g kg^{-1}. Northeastern Australia, northwestern Australia, southeastern China, northern India, the Caribbean, and south India (mostly bottom row) are 'moist' regions where regional mean summertime specific humidity is greater than 15 g kg^{-1}.

exceedance is 31 and 13% in northeast China but only 11 and 2% in southwest Australia. The impact of warming also varies, with southwest Australia reaching 95% exceedance of the 28 °C threshold for a warming of 5 °C, but with northeast China reaching only 88%. While these two regions experience a similar climatological W, they have distinctly different climates with northeast China being predominantly warm and moist and southwest Australia predominantly warm and dry (compare Figures 6 and 7). Of note also is the difference between exceedance of pentad W_{mm} relative to pentad $\overline{W}_m$ between regions (shown as colours and triangles in Figure 6) highlighting the complex relationship between means and extremes.

A 2 °C global mean temperature rise has become a globally recognised mitigation target. As of summer 2009, 124 countries have committed themselves to preventing climate change beyond this threshold. These results can address the likely W_{vars} threshold exceedance under a 2 °C warming, with the caveats that warming is considered relative to 1974–2003 (rather than preindustrial), and that regional scales are considered which will depart somewhat from global means. For all regions except the UK and northwest USA a further 2 °C warming corresponds to more than 50% of summertime pentad W_{mm} exceeding the 28 °C threshold. For southeast USA, northern Australia, India, and the Caribbean, a 2 °C warming brings summertime exceedance of the 32 °C threshold above 90% for pentad W_{mm}, and very close to 90% for pentad $\overline{W}_m$. It makes pentad W_{mm} exceedance of the 35 °C threshold a possibility for all regions except the UK, although at less than 5% occurrence in France and northwest USA. Pentad $\overline{W}_m$ exceedance of 35 °C remains very low for France, northern USA and southern Australia.

A 5 °C regional warming will likely have severe impacts on heat extremes in all regions, bringing 35 °C threshold exceedance to the UK in pentad W_{mm} and $\overline{W}_m$, albeit for less than 1% of summertime pentads, and to at least 10% for all other regions. For UK summertime pentads, approximately 40% of pentad W_{mm} and 15% of pentad $\overline{W}_m$ are shown to exceed 28 °C. For southeast USA, northern Australia, India, and the Caribbean ∼100% of summertime pentads are shown to exceed 32 °C, and just under 100% (lower for southeast USA) are shown to exceed 35 °C both in W_{mm} and $\overline{W}_m$.

5.2. Taking the background climate of the fifteen regions into account

There are two important questions to ask. First, how do these projected increases in W_{vars} relate to present regional climate – are increases larger or smaller in

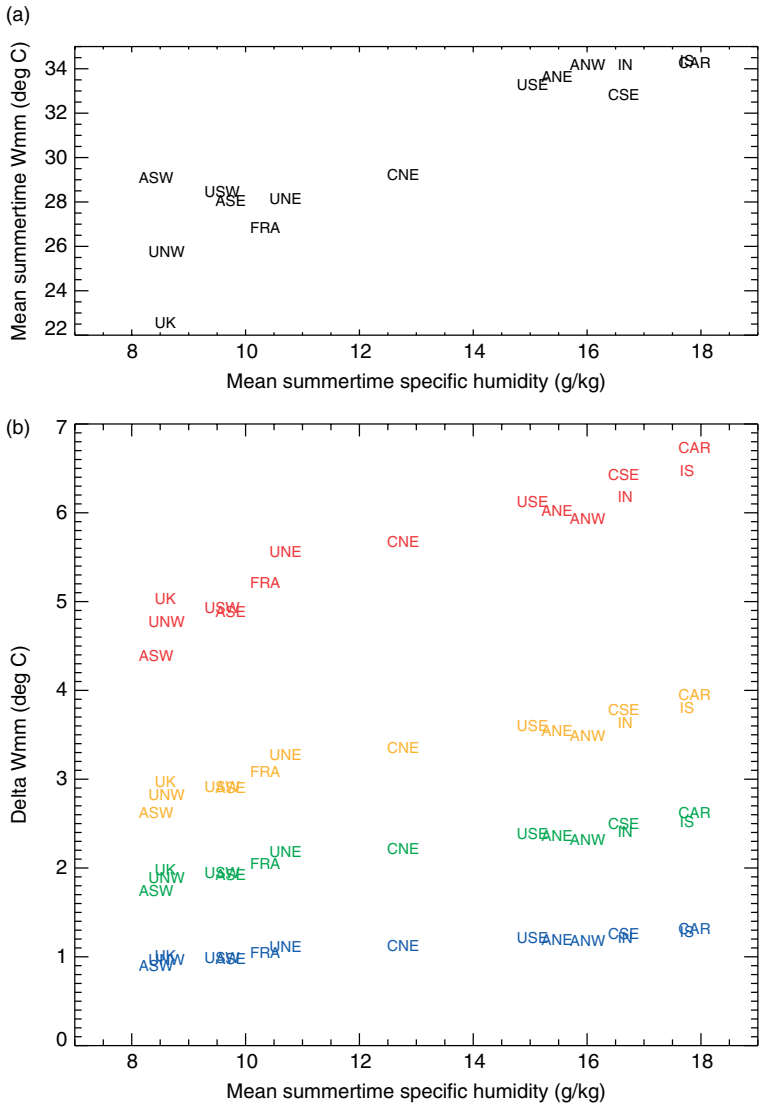

Figure 6. Comparison of the a) climatological (1974–2003) and b) projected change (blue = 1 °C, green = 2 °C, yellow = 3 °C, red = 5 °C) in summertime region mean W_{mm} against present-day region mean summertime specific humidity under a warming climate assuming constant relative humidity in 15 regions. To aid clarity, region names have been abbreviated as follows: UK = United Kingdom; FRA = France; UNW = Northwestern USA; UNE = Northeastern USA; USW = Southwestern USA; USE = Southeastern USA; ANW = Northwestern Australia; ANE = Northeastern Australia; ASE = Southeastern Australia; ASW = Southwestern Australia; IN = Northern India; IS = Southern India; CNE = Northeastern China; CSE = Southeastern China; and CAR = the Caribbean.

regions already experiencing the most stress? Second, how much future warming is expected in the regions under realistic emissions scenarios, and can regional changes in RH have a significant effect on the resulting changes in heat event character?

Figure 6a) and b) explores the relationship between $\mathrm{d}W/\mathrm{d}T$ (for W_{mm} calculated under the assumptions described above including constant RH) and mean summertime q for all regions. In general, humid regions experience the highest climatological W_{mm}, however, some regions like southwest Australia have a stronger influence of temperature over humidity relative to others. The UK, northwest USA and southwest Australia are comparably dry but the former two experience far lower W_{mm}. More moist regions experience a greater increase in W_{mm} per °C rise in temperature, as expected under the Clausius–Clapeyron relation. Similarly, this difference is non-linear, such that for 1, 2 and 5 °C T rises, under constant RH, the increase in W_{mm} of a humid region such as the Caribbean is greater than that for a less humid region such as southwest Australia (by 0.4, 0.9, and 2.34 °C, respectively).

The 15 regions represent a wide spread of climates and changes in climate over recent decades. Figure 7 summarises the present climate for each region in terms of the summertime trends of T, W and RH. This is shown alongside GCM projected change for an A1B scenario in T and RH, and W from present day (1974–2003 climate) to a 2020s and 2050s climate taking into account some model uncertainty. The assumption of constant RH can be tested, except for northern India, southeast China and France, none of the observed trends in summertime RH are significant and future projections for the most part are widely spread across zero. This suggests that the constant

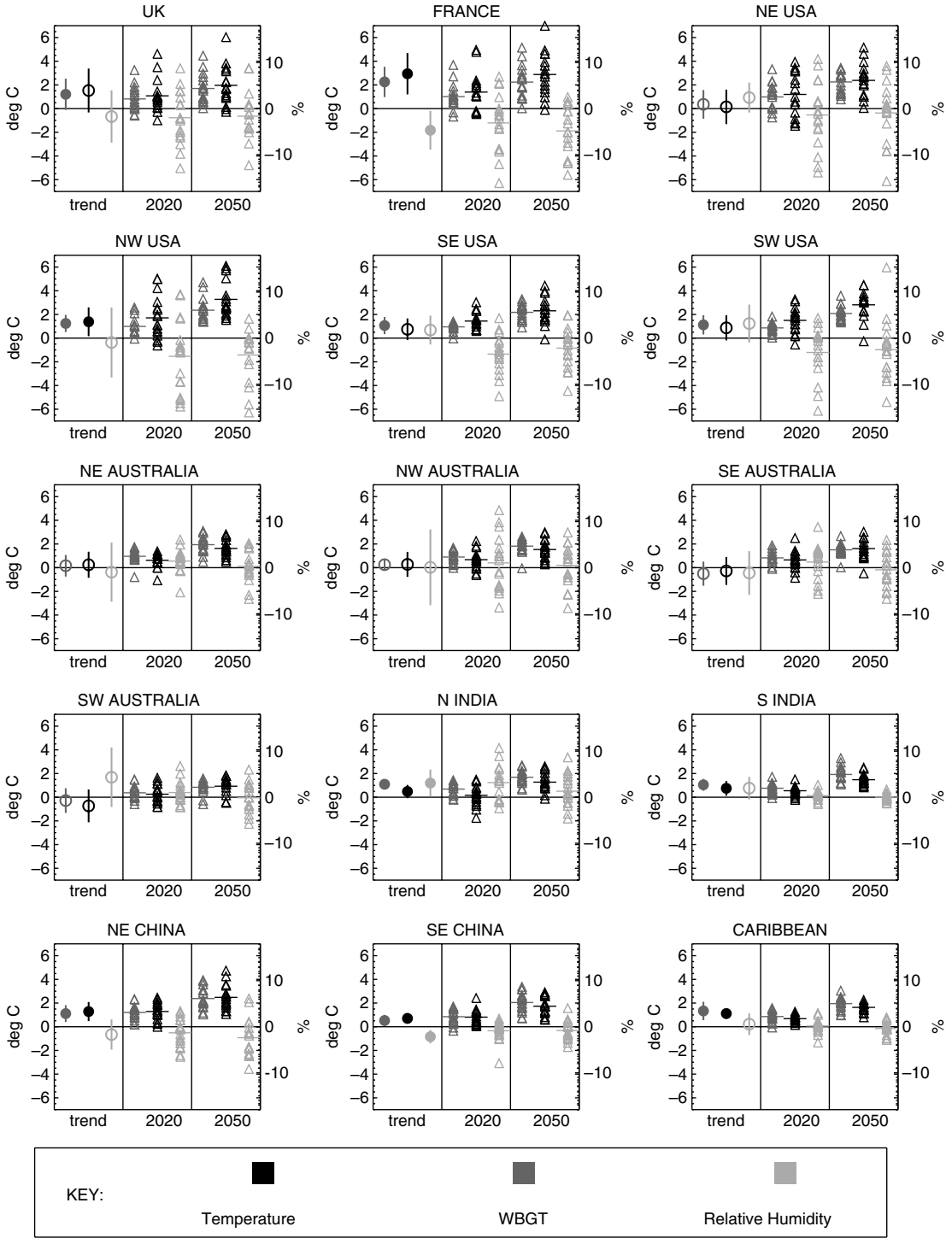

Figure 7. Assessing climatological characteristics for each region. Recent (1973–2003) decadal trends (circles with 2 SE error bars) in WBGT, temperature, and relative humidity (left axis). Projected climatological mean change relative to a 1974–2003 climatology in temperature, WBGT (middle axis) and relative humidity (right axis) for 2020 (2005–2034), and 2050 (2035–2064) from the QUMP (Collins *et al*., 2010) perturbed runs from HadCM3 under an A1B forcing scenario where bars identify ensemble mean and symbols represent individual runs. Recent trends are fitted as described in Table IV, and significance at 10% is shown by solid circles.

RH assumption is not an unreasonable one for most regions but that caution is necessary when interpreting results for some regions. Notably, model projections into future climates do not suggest that large *RH* trends will be sustained in any regions.

Recent trends in T and W are mostly positive with the exception of southern Australia, and significant for northwest USA, China, India, the Caribbean, and France ranging up to an increasing W of 2.9 °C 50 yr^{-1} and T of 2.2 °C 50 yr^{-1} in France. The decreasing *RH* over France is not sufficient to prevent a significant trend in W. Note that the large T *t*rends in France are affected by the extreme high temperatures in summer 2003 and the susceptibility of trends to extreme values near either

end of the record. Similarly, UK trends in T are not significant perhaps due to the very high summertime spike in 1976. Indeed, when these are calculated without 2003 and 1976, respectively, trends are slightly reduced over France and are slightly increased over the UK. This warns against overemphasising regional trend differences over only a few decades.

The ensemble means for all regions consistently project both increasing T and W for the 2020s and 2050s under an A1B scenario future. For southwest Australia and northern India the change in T for the 2020s is relatively evenly spread around zero implying strong uncertainty but by the 2050s warming is robustly predicted. The increasing T and W can be characterised in two ways. Firstly, for drier/mid-latitude stations the GCM ensemble projects decreasing RH which leads to larger increases in T than for W. Secondly, the more moist/tropical regions show near-constant RH or small increases and larger changes in W than T. To conclude, under an A1B scenario, future or similar, increases in T and W are largely consistent with our 1 to 3 °C analysis here. A 5 °C warming is more extreme than projected here.

The GCM ensemble mean for the mid-latitude UK projects rising W and T of the order of 1.7 and 2.0 °C, respectively, by 2050 (Figure 7). This is largely consistent with W_{mm} increases for the 2 °C temperature rise under constant RH discussed in this paper (Figures 5 and 6). This lifts the summertime pentad exceedance of the 32 °C threshold from 0.1 to 0.9%, and of the 35 °C threshold from 0.0 to 0.02%. For sub-tropical southeast USA the ensemble mean W and T increase by 2.2 and 2.3 °C, respectively, by 2050, again largely consistent with the projected W_{mm} changes under constant RH. This relates to a lifting of the exceedance level from 72.5 to 87.6% for the 32 °C threshold and from 21.6 to 64.8% for the 35 °C threshold. For tropical southern India a GCM ensemble mean rise in W and T of 1.9 and 1.5 °C, respectively, by 2050 is found which again is consistent with the projected W_{mm} increase. This infers a change from 82.2 to 92.6% and from 37.7 to 66.9% for the 32 and 35 °C thresholds (reading in between the values for a 1 and 2 °C warming). Notably, small islands are not well represented by the GCM due to the coarse land/sea mask and grid-box resolution. Consequently, warming over the Caribbean, for example, is likely to be underestimated. This can also be considered in terms of loss of labour productivity/activity where according to the recommended thresholds, a W exceedance of the 32 °C should reduce the amount of even light work to only 15 minutes for every hour above the threshold (Table III). It is not possible to say anything quantitative regarding productivity loss from this study due to the pentad resolution of the data, but this would make interesting future work utilising hourly data.

Changes in rainfall and RH have been identified as strong influences on regional warming rates, with relatively rapid warming expected in regions (including parts of Europe) that dry out, due to changes in Bowen ratio of surface fluxes caused by drier soils (Seneviratne *et al*., 2006). Such variations would have a partly cancelling effect on W; indeed, the spread of past and future changes in W shown in Figure 7 is generally smaller than the spread of changes in T, at least for the mid-latitudes. Thus, heat increases in future climates appear to be more predictable than increases in standard temperature.

Of further concern is the recent observation of significant changes in RH when extending the observational record out to 2007 (Simmons *et al*., 2010). It is beyond the scope of this study to extend the HadCRUH dataset and so the possibility of decreases in RH should be kept in mind. Ultimately, this should dampen the increases in W for a given rise in T.

6. Conclusions

In a warming and (for most regions) moistening globe over the recent decades, and highly likely into the future, an increase in the frequency and severity of heat events is clearly anticipated. Frequency of both single extreme event and extended periods of heat has increased in nearly all regions since 1973. Single events appear to have become more frequent relative to extended periods of heat in drier regions and vice versa in moist regions. The model presented here provides a simple and reasonable method for quantifying to first order how specific regions will fare under different levels of warming, assuming that WBGT distributions shift with little change in shape. The model does show statistically significant trend errors in a few locations, but is in good overall agreement with the observations. It seems to provide a reliable and useful tool to quantify regional exceedance of thermal comfort thresholds. All regions are shown to incur higher and more frequent high heat events in a warmer climate, but the rate and extent to which these increase under specific degrees of warming differs greatly region to region. Regions already experiencing considerable heat in terms of threshold exceedance become considerably worse in a warming climate.

Several calculations are presented that enable future changes in the rate of WBGT exceedence of key, activity-relevant thresholds to be estimated from given climatic changes. Specifically, the expected increases, given a local warming amount and the background specific humidity, are quantified, assuming relative humidity does not change. If changes in relative humidity are known or anticipated, these can be taken into account through a modest correction to the change in mean WBGT implied by the given change in temperature.

There are caveats with this model and methodology in addition to the small underestimation in the shift applied to region mean W due to calculation of humidity variables at coarse resolution. The W used here is simplified and will underestimate in full sun conditions and overestimate in very cloudy conditions. Therefore, for regions predisposed to either cloudy or clear sky climate there

may be some bias in the results and this should be taken into consideration. As a very broad example, sub-tropical regions such as central USA are likely to have proportionally more clear sky days whereas mid-latitude and especially west coast regions like the UK are likely to have proportionally more cloudy sky days. Also, the simple model given here is not adequate for very rare events (those events occurring only every few years or longer), where more sophisticated treatments of the distribution such as extreme value theory would be better. Our results should be quite reliable, however, for reasonably frequent events (exceedence rates of at least $\sim$5%).

Another issue is, the homogenised dataset presented here is not ideal, and a more thoroughly homogenised dataset at daily resolution and running up to the present is under development at the Hadley Centre. Also, the regions of study are large and heterogeneous in land use, elevation, aspect, and demographic structure. High-elevation stations have been removed to reduce the dampening effect of relatively cool high-elevation climates. A region mean approach will underestimate and overestimate for certain sub-regions and this should be recognised. In addition, China, India, and the Caribbean are studied over a six-month summer period due to their proximity to the ITCZ/passing overhead sun. This means that any percentage exceedance represents twice the duration compared to all other regions. This should also be taken into account should this method be used in any analysis including vulnerability both in terms of societal infrastructure, physiology, and economics.

The use of single event extremes (W_{mm}) and extended period extremes ($\overline{W}_m$) attempts to incorporate classical, occupational, and exertional heat stress in addition to heat-induced illness (described in Section 1). There are considerable implications for increased demands on emergency and health services in addition to both personal and industrial economic losses due to reduced working productivity from dangerous working conditions. The combination of economic loss and threshold exceedance is a potential future application of this model and methodology, especially as the thresholds coincide with recommended work levels.

How quickly (and indeed, *if*) regions reach 1, 2, 3, or possibly 5 °C of warming is still uncertain. Different regions will warm and experience modified moisture content at different rates. Furthermore, changes to urban fraction and composition, dominant vegetation type (arid or moisture loving), socio-economic factors influencing vulnerability and novel engineering strategies will differ hugely both within and between regions. However, we anticipate that our statistical results could be used to assess likely changes in WBGT exceedance rates given any scenario of future summertime mean temperature and humidity that is forecast as climate models and emissions scenarios continue to evolve. Improved estimates of future warming at the mesoscale are anticipated when regional models incorporate urban development and interactive vegetation. An ability to quantify the thermal discomfort to be expected in a certain climate is important. However, heat stress and its effect on humans is a highly complex issue and it is essential to now work on quantifying the societal, ecological, political, and physiological factors involved (to name a few) from many other disciplines.

Acknowledgments

The authors acknowledge help and advice from members of the Met Office Hadley Centre, in particular, Peter Thorne and David Parker. They also acknowledge data provision (HadCRUH and HadCM3) from the Met Office Hadley Centre. This work was funded by Yale University, and Katharine Willett was partly supported by the Joint DECC and Defra Integrated Climate Programme - GA01101.

References

ABOM: About the WBGT and Apparent Temperature indices – Australian Bureau of Meteorology. http://www.bom.gov.au/info/thermal_stress/.

ACGIH. 1996. Threshold Limit Values for Chemical Substances and Physical Agents and Biological Exposure Indices (1996–1997). American Conference of Governmental Industrial Health, Cincinnati, OH, USA.

ACSM. 1984. Prevention of thermal injuries during distance running. American College of Sports Medicine. *Medical Journal of Australia* **141**: 876–879.

Alexander LV, Zhang X, Peterson TC, Caesar J, Gleason B, Klein Tank AMG, Haylock M, Collins D, Trewin B, Rahimzadeh F, Tagipour A, Rupa Kumar K, Revadekar J, Griffiths G, Vincent L, Stephenson DB, Burn J, Aguilar E, Brunet M, Taylor M, New M, Zhai P, Rusticucci M, Vazquez-Aguirre JL. 2006. Global observed changes in daily climate extremes of temperature and precipitation. *Journal of Geophysical Research* **111**: D05109. DOI:10.1029/2005JD006290.

Allen. MR, Ingram WJ. 2002. Constraints on future changes in climate and the hydrological cycle. *Nature* **419**: 224–232.

Barnett AG, Tong S Clements A. 2010. What measure of temperature is the best predictor of mortality? *Environmental Research* **110**(6): 604–611.

Borden KA, Cutter SL. 2008. Spatial patterns of natural hazards mortality in the United States. *International Journal of Health Geographics* **7**: 64.

Buck AL. 1981. New equations for computing vapour pressure and enhancement factor. *Journal of Applied Meteorology* **20**: 1527–1532.

Cochrane D. Orcutt GH. 1949. Application of least squares regression to relationships containing auto-correlated error terms. *Journal of the American Statistical Association* **44**: 32–61.

Collins M, Booth BBB, Bhaskaran B, Harris GR, Murphy JM, Sexton DMH, Webb MJ. 2010. Climate model errors, feedbacks and forcings: A comparison of perturbed physics and multi-model ensembles. *Climate Dynamics*. DOI:10.1007/s00382-010-0808-0.

Dai A. 2006. Recent climatology, variability, and trends in global surface humidity. *Journal of Climate* **19**: 3589–3606.

Davis RE, Knappenberger PC, Michaels PJ, Novicoff WM. 2003. Changing heat-related mortality in the United States. *Environmental Health Perspectives* **111**(14): 1712–1718.

Donaldson GC, Keatinge WR, Saunders RD. 2003. Cardiovascular responses to heat stress and their adverse consequences in healthy and vulnerable human populations. *International Journal of Hyperthermia* **19**(3): 225–235.

Elliott WP. 1995. On detecting long-term changes in atmospheric moisture. *Climate Change* **31**: 341–367.

Falk B. 1998. Effects of thermal stress during rest and exercise in the paediatric population. *Sports Medicine* **25**(4): 221–240.

Gleason KL, Lawrimore JH, Levinson DH, Karl TR. 2008. A revised US climate extremes index. *Journal of Climate* **21**: 2124–2137.

Grimmond S. 2007. Urbanization and global environmental change: local effects of urban warming. *Geographical Journal* **173**: 83–88.

Hajat S, Armstrong B, Baccini M, Biggeri A, Bisanti L, Russo A, Paldy A, Menne B, Kosatsky T. 2006. Impact of high temperatures on mortality: is there an added heat wave effect? *Epidemiology* **17**(6): 632–638.

Hoppe P. 1999. The physiological equivalent temperature – a universal index for the biometeorological assessment of the thermal environment. *International Journal of Biometeorology* **23**: 71–75.

Hunter CH, Minyard CO. 1999. Estimating Wet Bulb Globe Temperature Using Standard Meteorological Measurements, WSRC-MS-99-00757, Westinghouse Savannah River Company: Aiken, SC.

Ishigami A, Hajat S, Kovats RS, Bisanti L, Rognoni M, Russo A, Paldy A. 2008. An ecological time-series study of heat related mortality in three European cities. *Environmental Health* **7**(5): 1–7.

IPCC. 2007. *Climate Change 2007: The Physical Science Basis*, Contribution of Working Group 1 to the Fourth Assessment Report of the Intergovernmental Panel on Climate Change. Solomon S, Qin D, Manning M, Chen Z, Marquis M, Averyt KB, Tignor M and Miller HL (eds), Cambridge University Press: Cambridge, pp 18.

ISO. 1989. *Hot Environments – Estimation of the heat stress on working man, based on the WBGT-index (wet bulb globe temperature)*. ISO Standard 7243. Geneva: International Standards Organization.

Katavoutas G, Theoharatos G, Flocas HA, Asimakopoulos DN. 2009. Measuring the effects of heat waves episodes on the human body's thermal balance. *International Journal of Biometeorology* **53**: 177–187.

Kenyon J, Hegerl GC. 2008. Influence of modes of climate variability on global temperature extremes. *Journal of Climatology* **21**: 3872–3889.

Kjellstrom T, Kovats RS, Lloyd SJ, Holt T, Tol RSJ. 2008. The direct impact of climate change on regional labour productivity. *ESRI* Working Paper No. **260**: 1–27.

Kovats RS, Hajat S, Wilkinson P. 2007. Contrasting patterns of mortality and hospital admissions during hot weather and heat waves in Greater London, UK. *Occupational Environmental Medicine* **61**: 893–898.

Kovats RS, Hajat S. 2008. Heat stress and public health: a critical review. *Annual Review of Public Health* **29**: pp 41.

Knight DB, Davis RE, Sheridan SC, Hondula DM, Sitka LJ, Deaton M, Lee TR, Gawtry SD, Stenger PJ, Mazzei F, Kenny BP. 2008. Increasing frequencies of warm and humid air masses over the conterminous United States from 1948 to 2005. *Geophysical Research Letters* **35**: L10702. DOI:10.1029/2008GL033697.

Kushner PJ, Held TL, Delworth TL. 2001. Southern hemisphere atmospheric circulation response to global warming. *Journal of Climate* **14**: 2238–2249.

Leighton B, Baldwin T. 2008. 2008 Australian Tennis Open. www.vailsala.com/files/2008_Australian_Tennis_Open.pdf.

Lott N, Baldwin P, Jones P. 2001. The FCC Integrated Surface Hourly database, a new resource of global climate data. National Climatic Data Center Technical Report. No. 2001-01, NCDC: Asheville, USA, pp 42.

Margolis HG, Gershunov A, Kim T, English P, Trent R. 2006. California heat wave high death toll: insights gained from coroner's reports and meteorological characteristics of event. *Epidemiology* **19**(6): S363–S364.

Masterson J, Richardson FA. 1979. *Humidex, A method of Quantifying Human Discomfort Due to Excessive Heat and Humidity*. Environment Canada: Downsview, Ontario, pp 45.

Mastrangelo G. 2006. Contrasting patterns of hospital admissions and mortality during heat waves: Are deaths from circulatory disease a real excess or an artefact? *Medical Hypotheses* **66**(5): 1025–1028.

McVicar TR, Van Niel TG, Li LT, Roderick ML, Rayner DP, Ricciardulli L, Donohue RJ. 2008. Wind speed climatology and trends for Australia, 1975–2006: capturing the stilling phenomenon and comparison with near-surface reanalysis output. *Geophysical Research Letters* **35**(20): L20403.

Meehl GA, Tebaldi C. 2004. More intense, more frequent, and longer lasting heat waves in the 21st century. *Science* **305**: 994–997.

Meehl GA. 2007. Global Climate Projections. In: *Climate Change 2007: The Physical Science Basis*. Contribution of Working Group I to the Fourth Assessment Report of the Intergovernmental Panel on Climate Change. Solomon S, Qin D, Manning M, Chen Z, Marquis M, Averyt KB, Tignor M and Miller HL (eds). Cambridge University Press: Cambridge, United Kingdom and New York, NY, USA.

Moran DS, Pandolf KB, Shapiro Y, Heled Y, Shani Y, Mathew WT, Gonzalez RR. 2001. An environmental stress index (ESI) as a substitute for the wet bulb globe temperature (WBGT). *Journal of Thermal Biology* **26**: 427–431.

O'Neill MS, Ebi KL. 2009. Temperature extremes and health: impacts of climate variability and change in the United States. *Journal of Occupational and Environmental Medicine* **51**: 13–25.

Parsons K. 2006. Heat stress standard ISO 7243 and its global application. *Industrial Health* **44**: 368–379.

Rothfusz LP. 1990. *The Heat Index Equation, SR Technical Attachment, 94–19*, pp 6.

Santer BD, Mears C, Wentz FJ, Taylor KE, Gleckler PJ, Wigley TML, Barnett TP, Boyle JS, Bruggermann W, Gillett NP, Klein SA, Meehl GA, Nozawa T, Pierce DW, Stott PA, Washington WM, Wehner MF. 2007. Identification of human-induced changes in atmospheric moisture content. *Proceedings of the National Academy of Sciences in the United States of America* **104**(39): 15248–15253.

Seneviratne SI, Luthi D, Litschi M, Schar C. 2006. Land-atmosphere coupling and climate changes in Europe. *Nature* **443**: 205–209.

Simmons AJ, Willett KM, Jones PD, Thorne PW, Dee D. 2010. Low-frequency variations in surface atmospheric humidity, temperature and precipitation: Inferences from reanalyses and monthly gridded observational datasets. *Journal of Geophysical Research* **115**: D01 : 110, DOI:10.1029/2009JD012442.

SMA: – Sports Medicine Australia – www.sma.org.au/information/heat.asp.

Sparks J, Changnon D, Starke J. 2002. Changes in the frequency of extreme warm-season surface dewpoints in northeastern Illinois: Implications for cooling-system design and operation. *Journal of Applied Meteorology* **41**(8): 890–898.

Steadman N. 1984. A universal scale of apparent temperature. *Journal of Climate and Applied Climatology* **23**: 1674–1687.

Steadman N. 1994. Norms of apparent temperature in Australia. *Australian Meteorology Magazine* **43**: 1–16.

Taylor NAS. 2006. Challenges to temperature regulation when working in hot environments. *Industrial Health* **44**: 331–344.

Trenberth KE, Fasullo J, Smith L. 2005. Trends and variability in column-integrated atmospheric water vapor. *Climate Dynamics* **24**: 741–758.

USARIEM: *U.S. Army Research Institute of Environmental Medicine* http://www.usariem.army.mil/heatill/precenhi.htm.

Wallace RF, Kriebel D, Punnett L, Wegman DH, Wenger CB, Gardner JW, Kark JA. 2006. Risk factors for recruit exertional heat illness by gender and training period. *Aviation, Space and Environmental Medicine* **77**(4): 415–421.

Wei WS. 1990. *Time Series Analysis: Univariate and Multivariate Methods*. Addison-Wesley Pub.: California, pp 496.

Wentz FJ, Ricciardulli L, Hilburn K, Mears C. 2007. How much more rain will global warming bring? *Science* **317**: 233–235.

Willett KW, Gillett NP, Jones PD, Thorne PW. 2007. Attribution of observed humidity changes to human influence. *Nature* **449**: 710–712.

Willett KW, Jones PD, Gillett NP, Thorne PW. 2008. Recent changes in surface humidity: development of the HadCRUH dataset. *Journal of Climate* **21**: 5364–5383.

Yaglou CP, Minard D. 1957. Control of heat casualties at military training centers. *Archives of Industrial Health* **28**: i–x.

UNFPA. 2007. *State of the World Population 2007*, UNFPA: pp 108.

